

A simple turbulence simulator for adaptive optics

Sandrine Thomas

Cerro Tololo Inter-American Observatory, Casilla 603, La Serena, Chile.

ABSTRACT

In this article, I describe a new, inexpensive way to make transparent phase screens. I list available technologies of physical turbulence simulation and describe the transparent phase-plate screens that were produced by the laquer-spray technique and characterized in the laboratory. The spatial spectrum of phase perturbations is a reasonable match to the Kolmogorov law with r_0 around 0.5 mm at $0.633 \mu\text{m}$ over spatial frequencies from 0.75 to 5 mm^{-1} . A turbulence simulator using two such rotating screens and destined for the adaptive optics instrument for the 4.1-m SOAR telescope is described.

Keywords: Phase screens, turbulence simulation, adaptive optics

1. INTRODUCTION

While the adaptive optics (AO) community fights daily to correct the distortions introduced by the atmosphere or by the liquid inside eyes, I concentrated my efforts in making physical turbulence simulators to create those perturbations. Such physical turbulence simulators are needed for engineering work and optimization of adaptive optics (AO) instruments. TurSim is the turbulent simulator designed for SAM (SOAR Adaptive Module)⁷ and consists of a telescope emulation with transparent turbulent phase screens in its pupil. In this article the results of the characterizations of such phase screens are given, as well as some details on the optical and mechanical design of TurSim.

Over the past few decades, the need for phase screens in astronomy increased with the number of AO systems. Several different technologies using both reflective and refractive methods have been developed. They have been nicely reviewed by Butler.¹ In the reflective category, one finds deformable mirrors (DM), liquid crystal modulators^{2,3} (LC) or rotating mirrors with distorted surfaces.⁴ DM and LC are also used as correctors and have given so far satisfactory results. However transmissive phase screens have the advantage of leading to more compact simulators, especially when more than one layer is considered. The first and natural technique is to use fluid simulators – with air or water – which are practically complex. Clever ideas such as photosculpture,⁵ laser writing, near index matching,⁶ sodium-silver ion exchange,¹ have been explored with success.

The drawback of those techniques is either their high cost and/or their complexity. Therefore, I focused myself on easy ways to make cheap phase screens and discovered that a phase plate of reasonable characteristics can be fabricated by depositing multiple layers of ordinary hair spray onto a glass substrate.

2. PHASE SCREENS FABRICATION

The fabrication of the phase plates is fast but requires some care. I fabricated the phase screens by spraying multiple layers of ordinary hair spray onto a glass substrate. I have used disks of glass from Rolyne pyrex^{*} and Hair Spray from Schwarzkopf with good results though many brands give similar results. This product contains a component called Amphomer[†], which resembles a resin. The protection of the Amphomer layer is achieved using another disc put in front of the first one and separated by circular shims. It is sealed under the pressure of an outside mechanical rings as shown in Figure 7.

Further author information: (Send correspondence to S.T.)

S.T: E-mail: sthomas@ctio.noao.edu, Telephone: 56 51 205 325

^{*}glass discs: stock 55.1100 Dia 3"; Thick 1/8" (www.rolyn.com)

[†]Octylacrilamide/Acrylates/Butylaminoethyl Methacrylate, <http://www.personalcarepolymers.com/Site/>

3. PHASE SCREEN CHARACTERIZATION

I characterize the phase screens by measuring the value of the r_0 with three methods: the modal representation, the power spectrum representation and the optical transfer function. The turbulence model used is based on the Kolmogorov law as explained below. In this paper I will show the results for two phase screens called PS1 and PS2. The different studies have been done independently, leading to different values for the pupil diameter specified each time.

3.1. Qualitative study

The distribution of Optical Path Difference (OPD) created by the phase screens in the exit pupil plane is shown in Figure 1. The qualitative appearance of it confirms the expectations: the perturbations are displayed in patterns approximatively circular, characteristic of an image of the pupil seen through a telescope. It is shown further that the Fried diameter is equal to about $500 \mu\text{m}$. Figure 1 represents the OPD obtained with a Shack-Hartmann wavefront sensor. On this figure, the Fried diameter would correspond to 5 pixels which is consistent with the observation.

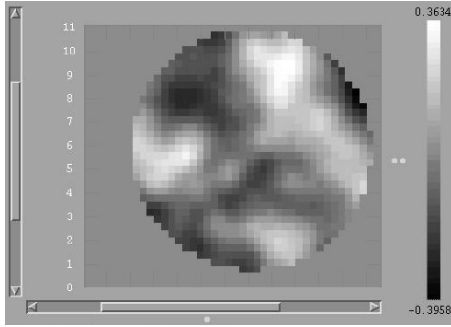


Figure 1. Optical Path Difference of one of the phase screens introduced in the beam. I used Wavescope with a $300 \mu\text{m}$ lenslet array. The pupil diameter is 3.4 mm on the phase screens. The tip/tilt and focus is removed. The OPD scale in microns is shown on the right.

In the focal plane, the behavior of the distortions of the image due to the phase screens looks like the “seeing”, as shown in Figure 2. The size of the spot image increases when going from no phase plate to one phase plate and then two phase plates, while the size of the speckles remains constant. As a first approximation, I can calculate the Fried diameter from those Point Spread Functions by measuring the size of the spot image which would be $\approx \lambda/r_0$. In the middle image, corresponding to the use of PS2, $D/(r_0)_1 \approx 12$ and on the right image, corresponding to the use of PS1 and PS2, $D/(r_0)_2 \approx 27$. In this set-up $D = 8 \text{ mm}$ leading to $(r_0)_1$ of about 660 microns and $(r_0)_2$ of about 300 microns .



Figure 2. Image of a monochromatic point source with the simulated telescope. These graphs show, from left to right, the degradation of the image quality when putting 0, 1 and then 2 phase plates in the beam. The aperture is about 8 mm on the phase screen for a $r_0 \approx 500 \mu\text{m}$. Different intensity scale for different configurations improves the contrast. $\lambda = 633 \text{ nm}$.

I will show in the following that all three methods demonstrate a reasonable match of our phase screens to the Kolmogorov law. The average measured value of r_0 over 6 disks is $500 \pm 100 \mu\text{m}$. The uncertainty is due to the imperfect homogeneity of the phase screens leading to variations of r_0 over the disk. Two phase disks, put one after the other, are used in the final turbulence simulator. If $(r_0)_1$ and $(r_0)_2$ are the Fried diameters for each disk, the resulting r_0 is computed by:

$$r_0 = [(r_0)_1^{-5/3} + (r_0)_2^{-5/3}]^{-3/5}. \quad (1)$$

For instance, if $(r_0)_1 = (r_0)_2 = 500 \mu\text{m}$, $r_0 \approx 330 \mu\text{m}$.

3.2. A modal expansion on Zernike basis

In the modal method,¹⁰ a wavefront can be decomposed by using a series of orthogonal functions. Here, the wavefront distortions are expanded in terms of the Zernike basis $Z_i(r)$. Thus the phase $\varphi(r)$ can be computed by:

$$\varphi(r) = \sum_i a_i Z_i(r). \quad (2)$$

Although other decompositions are also used the Zernike expansion is the most common. Knowing the telescope diameter D and the Fried diameter r_0 , one gets the rms values of atmospheric Zernike Coefficients $\langle a_i^2 \rangle$ using:

$$\sqrt{\langle a_i^2 \rangle} = \sqrt{N_i} * (D/r_0)^{5/6}, \quad (3)$$

where a_i are in radians and N_i are the Noll Coefficients.⁸ Inversely, knowing the Zernike expansion of any distorted wavefront over a circular aperture of unit radius, one can deduce the Fried parameter r_0 from $\langle a_i^2 \rangle$ for each order i . For a Kolmogorov phase screen, the same value of r_0 is expected for the different Zernike mode.

The measurements were made with the Wavescope Shack-Hartmann Wavefront sensing system[‡] over 20 positions on the screen and tip/tilt and focus were removed. The lenslet pitch was $300 \mu\text{m}$. The graphs of Figure 3 shows the measured r_0 as a function of the 40 first coefficients, as well as the mean r_0 .

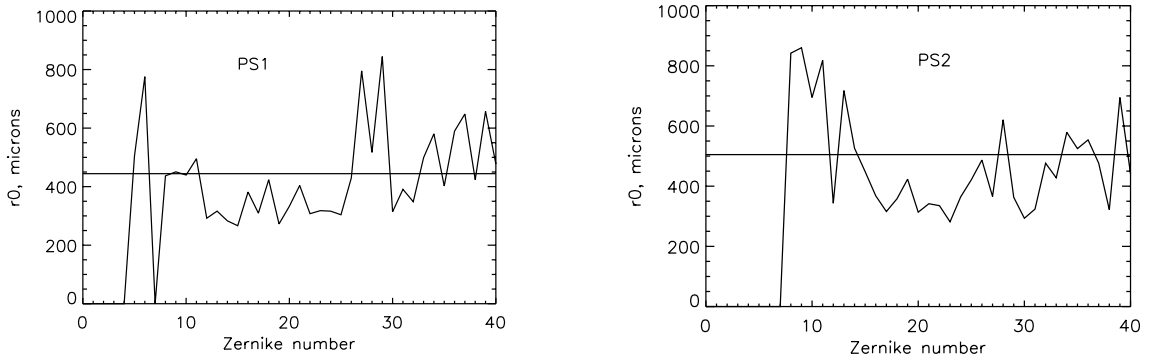


Figure 3. Graphs showing the quasi-Kolmogorov behavior of the phase screens using the decomposition over the Zernike polynomials. The resulting mean value for r_0 is about $450 \mu\text{m}$ for PS1 (left graph) and about $500 \mu\text{m}$ for PS2 (right graph).

The behavior is quasi-Kolmogorov expect for the first 4 Zernikes, due to the outer scale. The resulting r_0 is about $450 \pm 200 \mu\text{m}$ for PS1 and about $500 \pm 200 \mu\text{m}$ for PS2.

[‡]from AOA, Adaptive Optics Associates. <http://www.aoainc.com>

3.3. Power spectrum calculation

Another way to estimate the Fried parameter is to measure the power spectrum of the phase distortions. Indeed, the relationship between the phase fluctuations power spectrum $W(\mathbf{f})$ and the Fried diameter r_0 is^{9,11}:

$$W(\mathbf{f}) = 0.0028 * r_0^{-5/3} f^{-11/3}, \quad (4)$$

where \mathbf{f} is the spatial frequency. $W(\mathbf{f})$ is related to the OPD δ , by $W(\mathbf{f}) = \alpha * \langle |FFT(\delta)|^2 \rangle * (\lambda/2\pi)^2$, where FFT is the Fast Fourier Transform, $\langle |FFT(\delta)|^2 \rangle$ is the spectral energy and α is the coefficient converting the spectral energy in power spectrum. A rapid study shows that $\alpha = N_{tot} * \tau^2$, where N_{tot} is the total number of pixels in the image and τ the size of the pixels. Using Equation (4) one obtains the Fried parameter r_0 as a function of \mathbf{f} . The resulting curve should be close to a constant. For this experiment, I also used Wavescope with the 300 μm pitch lenslet.

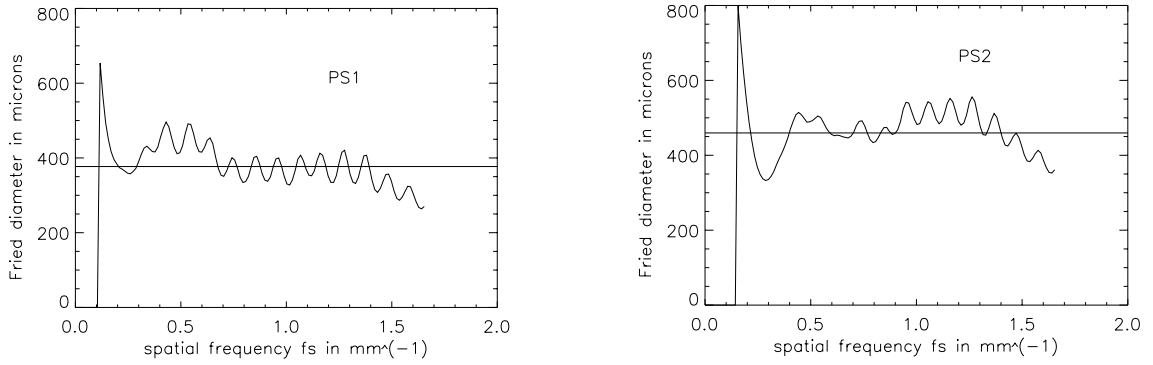


Figure 4. Graphs showing the quasi Kolmogorov spectrum of the phase screens. The resulting mean value for r_0 is about 400 μm for the left graph and about 460 μm for the right graph.

Figure 4 shows a plot of the r_0 versus the spatial frequency, calculated from the power spectrum. The behavior is quasi-Kolmogorov expect for very low frequencies, due to the outer scale. With this method, I find r_0 about $400 \pm 100 \mu\text{m}$ for PS1 and about $460 \pm 100 \mu\text{m}$ for PS2.

3.4. OTF

The normalized Optical Transfer Function (OTF) of a long exposure image is the Fourier Transform of its Point Spread Function (PSF) and can be expressed as:

$$OTF(\nu) = \exp[-3.44(\lambda\nu/r_0)^{5/3}], \quad (5)$$

where ν is the spatial frequency in the image plane in radians, λ the wavelength. The normalized OTF is computed from the PSF and r_0 is deduced from Equation (5) using $\nu_{1/e}$, where $OTF(\nu_{1/e}) = 1/e$.

The experiment was made with ST-7XE CCD camera from Sbig[§] with a pixel size equal to $\tau = 9 \mu\text{m}$. The phase screens are in a collimated beam brought to a focus by a lens with a focal $f_p = 100 \text{ mm}$. In order to get a better sampling, another lens was added in front of the CCD with a magnification of $m = 2.79$. Thus the sampling of the PSF is $s_{psf} = \tau/(mf_p) = 3.2 * 10^{-5} \text{ rad}$. The sampling for the OTF is then $s_{otf} = 1/(N * s_{psf}) \text{ rad}^{-1}$, where N is the size of the image in pixels.

From the $OTF(X)$ plot, where $X = \lambda\nu$ in μm (Figure 5), one measures the value of $X_{1/e}$ and gets the Fried diameter r_0 using $r_0 = 3.44^{3/5} X_{1/e}$. The resulting r_0 are gathered in the Table 1 for different configurations.

Using Equation (1), the resulting Fried diameter for the two phase screens is 369 microns, which is in the error bar of those measurements.

[§]Santa Barbara Instrument Group, <http://www.sbig.com>

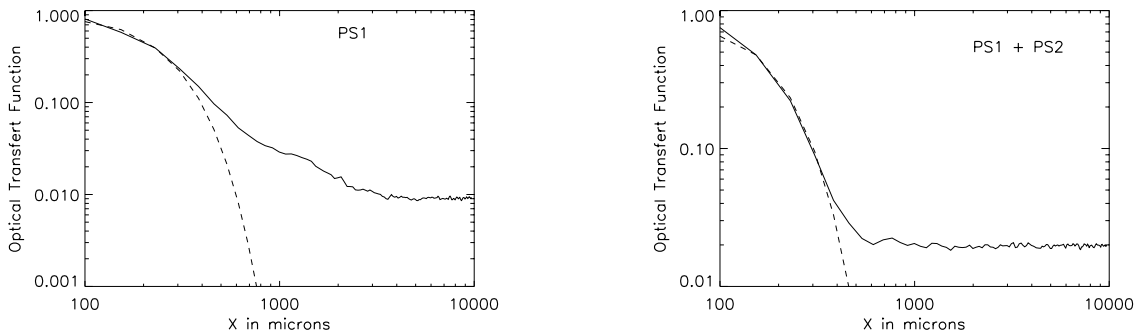


Figure 5. Optical Transfer Functions obtained when introducing one phase-screen in the beam – left graph – and two phase-screens – right graphs. The model given by Equation (5) is plotted in dashed line.

3.5. Summary

The three methods give similar results, within their uncertainties, as shown in Table 1.

Table 1. Summary the results for the three methods. r_0 is in microns

Method	PS1	PS2	PS1 and PS2 measured	PS1 and PS2 calculated
Zernike	450 ± 200	500 ± 200	*	312
Power spectrum	400 ± 100	450 ± 100	*	241
OTF	500 ± 100	660 ± 100	385 ± 100	374

In the following I will consider $(r_0)_{PS1} = 450 \mu\text{m}$ for PS1 and $(r_0)_{PS2} = 540 \mu\text{m}$ for PS2, leading to a total Fried diameter $(r_0)_{tot} = 320 \mu\text{m}$ at $0.633 \mu\text{m}$. The Fried diameter at $0.5 \mu\text{m}$ is then $241 \mu\text{m}$. We will consider the particular case of TurSim dedicated to simulate the atmospheric turbulence on Cerro Pachón where SOAR is located. The results of a site-testing campaign on Pachón¹² show that the average seeing is $0.67''$, which corresponds to $r_0 = 15 \text{ cm}$ at $0.5 \mu\text{m}$ at zenith. The diameter of the primary mirror of the SOAR telescope being 4.1 m , I need to simulate the turbulence with $D/r_0 \approx 27$ at $0.5 \mu\text{m}$. being 4.1 m , I need to simulate the turbulence with $D/r_0 \approx 27$ at $0.5 \mu\text{m}$. Therefore, the pupil diameter on the phase screen for the final instrument will be 6.6 mm .

4. OTHER CONSIDERATIONS

4.1. Scintillation

One interesting problem encountered in the use of turbulent phase screens is the scintillation. It is unavoidable since thick substrates are used. The thickness of the plates used in TurSim is 3 mm . The magnification factor between the disks and the simulated telescope pupil is $k = (r_0)_{tel}/(r_0)_{PS}$, where $(r_0)_{tel}$ correspond to the seeing on Cerro Pachón – 150 mm – and $(r_0)_{PS}$ is the Fried diameter of the phase screen – 0.24 mm . I find $k = 150/0.24 = 625$. Thus, taking 5 mm for the distance between one disk and the aperture, the distance in the simulated atmosphere will be $k^2 * 5 \text{ mm} = 1.95 \text{ km}$. The second layer of turbulence will be at about 13 mm from the aperture, e.g. 5.08 km for the simulated atmosphere. If the aperture is placed between the phase plates, the layers will be closer to the aperture, leading to less scintillation. I considered this acceptable, given that turbulence exists at such location in real life.

4.2. Tip/tilt produced by the phase screens

The tip/tilt has been studied also since TurSim is supposed to be placed after the SOAR mirror M3 which is the mirror chosen to correct the tip/tilt.⁷ This tip/tilt introduced by the phase plates has to be quite small to be either neglected or compensated by the deformable mirror itself.

This study has been done using the Zernike decomposition and Wavescope. The diameter of the pupil used to calculate the tip/tilt was 5.6 mm. The pupil diameter on the phase screens for the final instrument will be 6.6 mm. Using Equation (3), one can predict the tip/tilt introduced by the phase screens in TurSim $\langle a_i^2 \rangle_{tursim}$ knowing the measured Zernike coefficients $\langle a_i^2 \rangle_{meas}$ with: $\langle a_i^2 \rangle_{tursim} = \langle a_i^2 \rangle_{meas} * (D_{tursim}/D_{meas})^{5/3}$, where D_{meas} is the pupil diameter used in the measurement and D_{tursim} the one needed for the final instrument.

In average, $\sqrt{\langle a_{2,3}^2 \rangle_{meas}}$ is about 0.23 rad leading to $\sqrt{\langle a_{2,3}^2 \rangle_{meas}} = 0.26$ rad for a 6.6 mm aperture diameter. The Kolmogorov model claims that the tip/tilt rms error variance is $\sqrt{\langle a_{2,3}^2 \rangle_{theo}} = \sqrt{0.45 * (D/r_0)^{5/3}}$, which would be about 5.75 rad for $r_0 = 500 \mu\text{m}$ and $D = 6.6$ mm. The tip/tilt for the phase screen is 4% of the tip/tilt expected by the Kolmogorov model, thus negligible. This mismatch with the model is consistent with the previous results where the graphs (Figures 3 and 4) diverged from the theory for low Zernike modes and low frequencies.

5. IMPLEMENTATION

5.1. Optical design

As explained in Section 3.5, for an average value of r_0 of $240 \mu\text{m}$ at $0.5 \mu\text{m}$ for two phase screens, one needs a pupil diameter on the phase plate equal to about 6.6 mm in order to respect $D/r_0 \approx 27$ for the SOAR telescope.

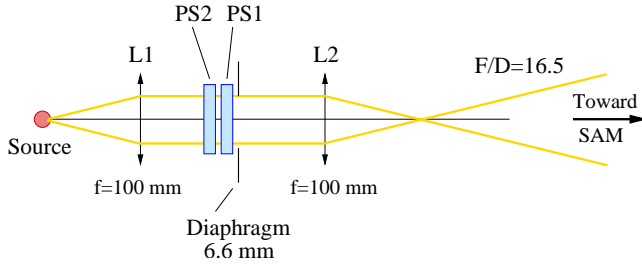


Figure 6. Scheme of the optical design for TurSim. The source will be changeable.

The extremely simple optical set-up is presented in Figure 6: a first lens collimates the beam coming from the source and the phase screens are introduced in this parallel beam. Moreover, in order to respect the f ratio of 16.5 of the SOAR telescope, the lens L2, imaging the pupil on the input of the SOAR AO instrument, has a focal length equal to about 100 mm. The pupil is defined by the diaphragm, disk with the spider and the central obstruction. The exit pupil of TurSim is at the same distance from the SOAR focal plane as the exit pupil of the SOAR telescope.

One can change the simulated seeing from median to good, using one or two phase plates. Worse seeing can be obtained by increasing the pupil diameter and changing the second imaging lens.

As said in the introduction, I plan to use both monochromatic and polychromatic sources. The monochromatic source will be either a laser diode or a UV LED directly mounted in the TurSim box. The LED UV will be used to align and test the wavefront sensor at about 355 nm, the wavelength of the Rayleigh laser guide star. The polychromatic source would be a white LED with a pinhole.

5.2. Mechanical considerations

From the MASS results¹³ of seeing measurements on Cerro Pachón, the median time constant is $\tau_s = 3.5$ ms, with possible values from 1 to 10 ms. The time constant is defined by $\tau = 0.31 * r_0/v_t$, where v_t is the speed of the turbulent layers. Thus for a median seeing $r_0 = 15$ cm, the required transversal speed of the phase screens is $v_t = 13.3 \text{ m.s}^{-1}$.

This is achieved by driving the disks with two DC Maxon Motors supplied from a voltage regulated source, to independently change the speed of the two phase screens. The position of the aperture on the phase screens relative to axis of the motors is 27.5 mm and the magnification between TurSim and the simulated atmosphere is $k \approx 625$ (section 4.1). Therefore, the required rotation period P of the motors is $1/P = (v_t/2\pi r)/k = 7.4$ RPM.

The two phase screens are mounted as shown in Figure 7 and the whole system is attached to a rigid small platform.

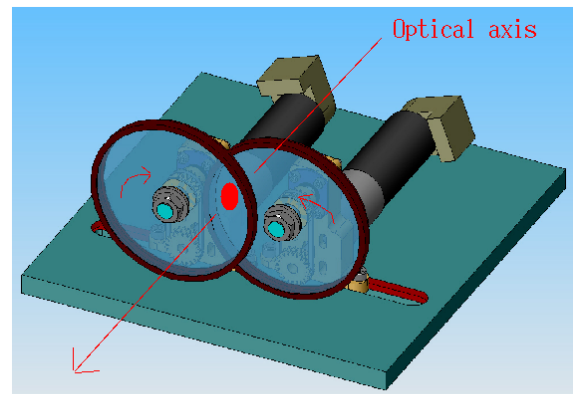


Figure 7. **Left** Pictures of the prototype installed in the laboratory. **Right** Global view of the support for the discs. Each disc is connected to its own DC motor, with variable speed.

Using two motors allows us have more flexibility on the direction and the speed of each disc and therefore get a better sampling of the turbulence statistic. One can obtain $(2\pi r/r_0)^2 = 11.8 \times 10^4$ independent instantaneous phase-screens. The size of the whole system can be put in a 300x300 mm box.

6. CONCLUSIONS

I discovered an easy way to build phase screens with an approximately Kolmogorov phase statistics. The r_0 obtained are about 500 μm and are fairly homogeneous. With the possibility of changing sources and only one lens, this instrument is a good emulation of the SOAR telescope and a good test for SAM. Moreover I can simulate different atmospheric conditions corresponding to good, median and bad seeing.

ACKNOWLEDGMENTS

I acknowledge Andrei Tokovinin for helping along the process of developing TurSim. I want to thank Roberto Tighe to help me in my experiments with Hair Spray, and my tests of different protections. I would like also to thank Patricio Schurter for his help on the mechanical part of this project.

REFERENCES

1. D.J. Butler, E. Marchetti, J. Bahr, W. Xu and S. Hippler, "Phase screens for astronomical multi-conjugate adaptive optics: application to MAPS", *Proc SPIE*, **4839**, pp. 623-634 2003.
2. P.M. Birch, J. Gourlay, N.P. Doble, A. Purvis, "Real time adaptive optics correction with a ferroelectric liquid crystal spatial light modulator and Shack-Hartmann wavefront sensor", *Proc SPIE*, **3126**, pp. 185-190, 1997.
3. L. Gordon, "Wavefront correction and production of Zernike modes with a liquid crystal spatial light modulator", *Appl. Opt.*, **36**, pp. 1517-1524, 1997.
4. B. Servan, Meudon Observatory, Phase screen using reflection components for NAOS, Private discussion.
5. R. Navarro and E. Moreno-Barriuso, "Phase plates for wave-aberration compensation in the human eye", *Opt. Lett.*, **25**, pp. 236-238, 2000.
6. T.A Rhoadarmer. and J.R.P. Angel, "Low-cost broadband static phase for generating atmosphericlike turbulence", *Appl. opt.*, **40**, pp. 2946-2955, 2001.
7. A. Tokovinin, S. Thomas, B. Gregory, N. van der Blik, P. Schurter, R. Cantarutti, E. Mondaca, "Design of ground-layer turbulence compensation with Rayleigh beacon", *Proc SPIE*, **5490**, paper 78, 2004.
8. R.J. Noll, "Zernike polynomials and atmospheric turbulence", *JOSA*, **66**, pp. 207-211, 1976.
9. J.W. Hardy, "Adaptive Optics for Astronomical Telescopes", *Oxford University Press*, 1998.
10. E. Gendron, "Modal control optimization in an adaptive optics system", *Active and Adaptive Optics*, ESO Conf. Garching, **48**, pp. 187-192, 1993.
11. F. Roddier, "Theoretical aspects", in "Adaptive Optics in Astronomy", *Cambridge University press*, pp. 25-56, 1999.
12. J. Vernin, A. Agabi, R Avila, M. Azouit, R. Conan, F. Martin, E. Masciadri, L. Sanchez, and A. Ziad, Gemini site testing campaign on Cerro Pachón and Cerro Tololo, *Gemini RPT-AO-G0094*, <http://www.gemini.edu/>, 2000.
13. A. Tokovinin, MASS Database, <http://www.ctio.noao.edu/atokovinin/profiler/index.html>